Title

Improvements in the synthesis and understanding of the iodo-bridged intermediate en route to the Pt(IV) prodrug satraplatin

Authors

Johnstone, Timothy C
Lippard, Stephen J

Publication Date

2015

DOI

10.1016/j.ica.2014.08.047

Peer reviewed

Published in final edited form as:
Inorganica Chim Acta. 2015 January 1; 424: 254–259. doi:10.1016/j.ica.2014.08.047.

Improvements in the Synthesis and Understanding of the Iodo-bridged Intermediate en Route to the Pt(IV) Prodrug Satraplatin

Timothy C. Johnstone and **Stephen J. Lippard***
Department of Chemistry, Massachusetts Institute of Technology, Cambridge, Massachusetts 02139, United States

Abstract

Mixed amine/ammine motifs are important features in newer generation platinum anticancer agents, including the Pt(IV) prodrug satraplatin. One synthetic route that can be used to access platinum molecules with such structures exploits the trans effect during NH_3-mediated cleavage of iodo-bridged platinum(II) dimers of the form $[Pt(Am)I(\mu\text{-}I)]_2$, where Am is an amine. A clear picture of the nature of these dimers that is consistent with the reactivity they exhibit has remained elusive. Moreover, technical aspects of this chemistry have impeded its more widespread use. We present here an improved strategy that permits isolation and use of $[Pt(Am)I(\mu\text{-}I)]_2$, where Am is cyclohexylamine, within minutes as opposed to weeks, as previously reported. A detailed spectroscopic, crystallographic, and chromatographic investigation of this intermediate in the synthesis of satraplatin is also presented with a discussion of the ability of both cis and trans isomers of the dimer to produce exclusively *cis*-$[Pt(NH_2C_6H_{11})(NH_3)I_2]$ upon treatment with NH_3.

Keywords

cisplatin; iodo-bridged dimer; multinuclear NMR; platinum anticancer agents; satraplatin

1. Introduction

Three square-planar platinum(II) complexes are currently approved by the US Food and Drug Administration for cancer treatment. Although much emphasis within the platinum anticancer drug research community has historically been placed on Pt(II) compounds, Pt(IV) species were identified as biologically active in some of the earliest reports [1]. These

*Correspondence to: lippard@mit.edu.

Supplementary material

Supplementary material includes NMR spectra and crystallographic information files. CCDC 1004061 and 1004062 contain the supplementary crystallographic data for *cis*-$[Pt(NH_2C_6H_{11})_2I_2]\cdot(CH_3)_2CO$ and $[Pt(NH_2C_6H_{11})I(\mu\text{-}I)]_2\cdot 2(CH_3)_2CO$. These data can be obtained free of charge from The Cambridge Crystallographic Data Centre via www.ccdc.cam.ac.uk/data_request/cif. Supplementary data associated with this article can be found, in the online version, at doi:XX.

studies eventually led to the clinical evaluation and approval of cisplatin. Although interest in Pt(IV) drug candidates has remained steady, this subdomain within the platinum anticancer field has recently seen a surge in activity [2,3]. Three Pt(IV) complexes, ormaplatin, iproplatin, and satraplatin (Chart 1), have entered human clinical trials [4]. Satraplatin, in combination with prednisone, was evaluated in a Phase III clinical trial for the treatment of hormone refractory prostate cancer [5].

One key feature of satraplatin is the mixed amine/ammine pharmacophore that is released upon reduction from Pt(IV) to Pt(II) [7,8]. This motif has been employed in a number of other compounds including a close relative of satraplatin, *c*,*c*,*t*-ammineadamantylamine-dichlorodiacetatoplatinum(IV), also known as LA-12 [9]. Mixed amine/ammine structures also occur in cycloplatam and picoplatin, Pt(II) compounds that have been entered into Phase II and III clinical trials, respectively [10-12].

Synthetic routes to access *cis*-ammine/amine platinum(II) compounds typically fall into one of two classes [3]. The first relies on the preparation of $[Pt(NH_3)Cl_3]^+$, which can undergo ligand substitution at one of the chlorides, often through an iodo intermediate, to afford *cis*-$[Pt(NH_3)(Am)Cl_2]$, where Am is an amine [13]. A second route (Scheme 1) involves the preparation of iodo-bridged platinum-amine dimers, which can be cleaved by NH_3 to give *cis*-$[Pt(NH_3)(Am)I_2]$ [14]. Silver-mediated iodide abstraction followed by incubation with chloride affords *cis*-$[Pt(NH_3)(Am)Cl_2]$. This latter method nicely exploits the trans effect, but technical aspects of the chemistry have hampered its widespread implementation. Details of the mechanism and intermediates have been a matter of debate [14-20].

Here we present a synthetic methodology that provides access to, and use of, the satraplatin intermediate $[Pt(NH_2C_6H_{11})I(\mu\text{-}I)]_2$ at a rate that is orders of magnitude faster than the currently employed methods and can be more readily monitored. Moreover, it produces fewer side products and avoids the generation of perchlorate salts. We have also carried out an in depth characterization of $[Pt(NH_2C_6H_{11})I(\mu\text{-}I)]_2$ that reconciles conflicting reports within the literature. This characterization rationalizes not only spectroscopic data but also the reactivity of this important synthetic intermediate.

2. Experimental

2.1. General considerations

Reagents and solvents were obtained from commercial vendors and used without further purification. *cis*-$[Pt(NH_2C_6H_{11})_2I_2]$ was prepared as previously described [21] and displayed spectra consistent with its proposed structure (Fig. S6–S8). NMR spectra were acquired on a Varian Inova-500 NMR spectrometer in the MIT Department of Chemistry Instrumentation Facility. ^1H and ^{13}C spectra were referenced to tetramethylsilane using residual solvent peaks and ^{195}Pt spectra were referenced to Na_2PtCl_6 using an external standard of K_2PtCl_4 in D_2O (δ –1628 ppm). ^{195}Pt NMR spectra were acquired with a 50 kHz (5000 ppm) scan width and represent the average of 3600 scans. Unless otherwise specified, NMR spectra were acquired at room temperature. Super-ambient variable temperature (VT) NMR experiments were performed using an Oxford VT controller driving an in-probe heater coil. Sub-ambient VT NMR experiments were performed using nitrogen

gas passed through a heat exchanging coil inside a Styrofoam bucket filled with liquid nitrogen at a rate of 10-15 L min^{-1}.

2.2. Synthesis of $[Pt(NH_2C_6H_{11})I(\mu\text{-}I)]_2$

cis-$[Pt(NH_2C_6H_{11})_2I_2]$ (100 mg, 0.16 mmol) was dissolved in acetone (10 mL) and tetrafluoroboric acid diethyletherate (30 μL, 0.19 mmol) was added. The mixture was stirred at room temperature for 5 h over which time the color of the reaction mixture changed from yellow to orange-red. The reaction volume was reduced to 5 mL under vacuum. Diethylether (50 mL) was added to precipitate an orange-brown solid, which was collected by filtration, washed with water, and dried overnight under vacuum. Yield: 68 mg (80%). Spectroscopic characterization matched that previously reported [21]. NMR spectra are reproduced in Fig. S3–S5. Analytical thin layer chromatography (TLC) was carried out on plastic plates coated with a 0.25 mm thick layer of silica gel 60. An acetone solution of $[Pt(NH_2C_6H_{11})I(\mu\text{-}I)]_2$ was spotted onto the plate and eluted with 1:5 ethylacetate:hexanes. The spot resolved into two bands with R_f values of 0.33 and 0.63. Preparative TLC was carried out on glass plates coated with a 1 mm thick layer of silica gel 60. The sample was applied as an acetone solution and eluted with 1:5 ethylacetate:hexanes. The bands were separated and the compound was extracted from the silica by adding acetone, filtering, and concentrating the filtrate under vacuum. The residue obtained from each band was analyzed by analytical TLC as described above, and each again gave rise to two spots with R_f values of 0.33 and 0.63.

2.3. UV-vis spectroscopic monitoring of the reaction of HBF_4 and cis-$[Pt(NH_2C_6H_{11})_2I_2]$

cis-$[Pt(NH_2C_6H_{11})_2I_2]$ (10 mg, 0.016 mmol) was dissolved in acetone (1 mL) and tetrafluoroboric acid diethyletherate (3 μL, 0.019 mmol) was added. An aliquot of the reaction mixture was immediately loaded into a solution IR cell outfitted with KBr windows and a Teflon spacer providing a path length of 0.1 mm. The cell was placed within the optical path of a Cary 50 UV-visible spectrometer and a spectrum was acquired. The reaction was allowed to proceed at room temperature in the dark. After 5 h, the cell was reloaded with a fresh aliquot of the reaction mixture and a spectrum was acquired. The reaction mixture was allowed to continuing stirring overnight at room temperature in the dark, after which another UV-vis spectrum was acquired in the manner described above. No change had occurred from the 5 h spectrum.

2.4. Variable temperature ^{195}Pt NMR spectroscopy of $[Pt(NH_2C_6H_{11})I(\mu\text{-}I)]_2$

A solution of $[Pt(NH_2C_6H_{11})I(\mu\text{-}I)]_2$ in acetone-d_6 was cooled to −70 °C and a separate DMF-d_7 solution of the compound was heated to 50 °C. In neither case was any change observed over the temperature range investigated (Fig. S1) with the exception of decomposition to Pt(0) and deposition of a platinum mirror on the NMR tube at temperatures greater than 70 °C.

2.5. NMR spectroscopic monitoring of the reaction of NH_3 (aq) and $[Pt(NH_2C_6H_{11})I(\mu\text{-}I)]_2$

A solution of $[Pt(NH_2C_6H_{11})I(\mu\text{-}I)]_2$ was prepared in acetone-d_6. A ^{195}Pt NMR spectrum was acquired. A drop of concentrated aqueous ammonia was added to the NMR tube and the

solution immediately changed color from orange-red to yellow. Another ^{195}Pt NMR spectrum was acquired.

2.6. Synthesis of cis-[Pt(NH$_2$C$_6$H$_{11}$)(NH$_3$)I$_2$]

[Pt(NH$_2$C$_6$H$_{11}$)I(μ-I)]$_2$ (68 mg, 0.062 mmol) was dissolved in acetone (6 mL) to afford an orange-red solution and concentrated aqueous ammonia (0.1 mL, approx. 15 mmol) was added. The color of the solution immediately changed to yellow. Water (10 mL) was added and the reaction was cooled on ice for 5 h to induce precipitation of a yellow solid. The solid was collected by filtration, washed with water, and dried under vacuum. Yield 46 mg (67%). Spectroscopic characterization matched that previously reported [22] (see Fig. 4 and S2).

2.7. X-ray crystallography

Crystals of [Pt(NH$_2$C$_6$H$_{11}$)I(μ-I)]$_2$·2(CH$_3$)$_2$CO were grown by slow evaporation of an acetone solution of the compound at −40 °C. Crystals of *cis*-[Pt(NH$_2$C$_6$H$_{11}$)$_2$I$_2$]·(CH$_3$)$_2$CO were grown by vapor diffusion of diethylether into an acetone solution of the compound. Samples suitable for X-ray diffraction were selected under crossed-polarizers, mounted on a nylon cryoloop in Paratone oil, and cooled to 100 K under a stream of nitrogen. A Bruker APEX CCD X-ray diffractometer controlled by the *APEX2* software was used to record the diffraction of graphite-monochromated Mo Kα radiation (λ = 0.71073 Å) [23]. The data were integrated with *SAINT* [24] and absorption, Lorentz, and polarization corrections were applied using *SADABS* [25]. Space group determination was carried out by analyzing the Laue symmetry and the systematically absent reflections with *XPREP* [26]. Structure solution via the heavy atom method and refinement were performed with the *SHELX-97* program suite [27,28]. Refinement was carried out against F^2 using standard procedures [29]. Non-hydrogen atoms were located in difference Fourier maps and refined anisotropically. Hydrogen atoms were placed at calculated positions and refined using a riding model. For terminal CH_3 groups, hydrogen atom isotropic displacement parameters (U_{iso}) were set equal to 1.5 times the U_{iso} of the atom to which they were attached. For other hydrogen atoms, U_{iso} = 1.2 U_{iso} of the attached atom. All structures were checked for missed higher symmetry and twinning with *PLATON* [30,31] and were further validated using *CheckCIF*. Refinement details are presented in Table 1.

3. Results and Discussion

3.1. Synthesis of [Pt(NH$_2$C$_6$H$_{11}$)I(μ-I)]$_2$

Treatment of *cis*-[Pt(Am)$_2$I$_2$] with perchloric acid in water, or a water-ethanol mixture, results in protonation and subsequent loss of an amine ligand [18]. This ligand dissociation reaction leads to dimerization, which is driven by the proclivity of the iodide ligand to bridge two soft Pt(II) centers. When Am is cyclohexylamine, as required to prepare satraplatin, neither the *cis*-[Pt(Am)$_2$I$_2$] starting material nor the [Pt(Am)I(μ-I)]$_2$ product is soluble in water. The reaction, as previously carried out, proceeds as a suspension that gradually changes from yellow to orange-brown [15]. Because of the suspension, is difficult to assess the degree of completion of the reaction, but if aliquots are periodically removed and analyzed by ^{195}Pt NMR spectroscopy, then it can be appreciated that the reaction occurs on the time scale of days to weeks. We observed that the reaction can be carried out much

more readily in an organic solvent, such as acetone, using an acid with a non-coordinating conjugate base, such as HBF_4. Similar results were also obtained using trifluoroacetic acid (data not shown). The starting materials and products are completely soluble, permitting the chemistry to proceed much more rapidly than the previously reported methods [18]. Over the course of 5 h, the yellow solution of *cis*-$[Pt(NH_2C_6H_{11})_2I_2]$ turns orange-red, allowing the reaction to be followed by UV-vis spectroscopy (Fig. 1).

Addition of water to the orange-red solution generates an orange-brown precipitate. The spectroscopic properties of solutions of this solid match those reported for the material obtained using the aqueous perchloric acid method described above. The combustion analysis previously reported for the compound is consistent with its formulation as an iodo-bridged dimer having the composition $[Pt(NH_2C_6H_{11})I(\mu\text{-}I)]_2$ [14].

In previous discussions in the literature, the spatial arrangement of the atoms in the dimer, notably the relative disposition of the two cyclohexylamine ligands (Scheme 1) has been referred to using the cis-trans nomenclature. In the trans configuration, the two cyclohexylamine ligands are each cis to a different bridging iodide ligand, whereas the cis configuration of the dimer places both cyclohexylamine ligands cis to the same bridging iodide (Scheme 1). Although it is often common to refer to this distinction using the syn-anti terminology, no explicit recommendation is provided by IUPAC [32]. The use of the cis-trans terminology parallels the s-cis and s-trans terminology used to describe syn-periplanar and anti-periplanar configurations [33]. Moreover, use of the cis-trans descriptors as indicated above allows the syn-anti descriptors to be used to denote different conformational isomers of the dimer, as described in greater detail below.

3.2. Spectroscopy and reactivity of $[Pt(NH_2C_6H_{11})I(\mu\text{-}I)]_2$

Initially, the dimer was proposed to exist solely as the trans species because of the reactivity it exhibited upon addition of ammonia; the dimer is cleaved to afford exclusively *cis*-$[Pt(NH_2C_6H_{11})(NH_3)I_2]$ according to the prediction depicted in Fig. 2 [14,15]. Cleavage of the cis dimer was predicted to afford one equivalent of the desired *cis*-amine/ammine and one equivalent of the undesired *trans*-amine/ammine (Fig. 2) [15]. Because the cis isomer was the major product obtained from the reaction mixture, the dimer was proposed to exist exclusively in the trans form. It should be noted that, in these previous discussions, the mechanism of the proposed ligand substitution was not discussed; the dashed lines in Fig. 2 and analogous diagrams [14] simply indicate which bonds are proposed to be broken during the course of the reaction

Spectroscopic evidence, however, does not support this reasoning. NMR spectra of solutions of the dimer show multiple sets of peaks for each of the various NMR active nuclei [18]. This feature is most clearly displayed in the ^{195}Pt spectrum of the compound, which contains two well-defined, baseline-resolved peaks (Fig. 4a). These signals, reported previously [15], were attributed to a “subtle electron density difference between the two [formally equivalent] platinum atoms.” Our work on the conformational isomerism of *trans*-$[Pt(NH_2C_6H_{11})_2I_2]$ suggests that restricted rotation of the cyclohexylamine groups about the dimer coordination plane, producing syn and anti conformers (Fig. 3), is not the origin of the two signals in the ^{195}Pt NMR spectrum of $[Pt(NH_2C_6H_{11})I(\mu\text{-}I)]_2$ [34].

A recent report describes the production of varying amounts of trans mononuclear platinum complexes from cleavage of the iodo-bridged dimer [35]. These results were interpreted to indicate the presence of the cis isomer of the dimer, consistent with the presence of the two ^{195}Pt NMR signals. These reactions, however, were carried out over a period of 2–70 days, as required in order for the starting material to be fully consumed owing to the heterogeneous nature of the reaction [35]. In these instances, we anticipate that the cis product will initially form but isomerize to the trans complex over the course of the long reaction time. Such isomerization reactions are well-documented [36].

On the other hand, addition of excess NH_3 (aq) to an acetone solution of the dimer results in an immediate change in color from orange-red to yellow. ^{195}Pt NMR spectra acquired before and after addition of NH_3 show clean conversion of the −4017 and −4030 ppm signals from the dimer to a single resonance at −3337 ppm (Fig. 4). Additionally, the ^{1}H NMR spectrum clearly shows the presence of only one isomer in the product (Fig. S2). This reaction can also be carried out on a preparative scale and, again, a single isomer is formed.

3.3. Crystal structures of cis-$[Pt(NH_2C_6H_{11})_2I_2]\cdot(CH_3)_2CO$ and $[Pt(NH_2C_6H_{11})I(\mu\text{-}I)]_2\cdot 2(CH_3)_2CO$

The crystal structure of the acetone solvate of *cis*-$[Pt(NH_2C_6H_{11})_2I_2]$ (Fig. 5) reveals a complex having a typical square-planar geometry at platinum and two cyclohexyl group from the amine ligands arranged on the same side of the platinum coordination plane. This sterically hindered conformation allows the amine groups to hydrogen bond to the iodide ligands of an adjacent molecule. The structures of a number of other *cis*-diaminediiodoplatinum(II) compounds containing primary amines have been solved [37-46]. In the analogous dicyclopentylamine complex, the two hydrocarbon groups are disposed anti to one another [41].

When an acetone solution of the dimer is allowed to evaporate slowly at –40 °C, red diffraction-quality crystals form. An X-ray crystallographic analysis of these prisms reveals the structure of the acetone solvate of the trans isomer of the dimer (Fig. 5). The dimer sits on a crystallographic inversion center and as a consequence, the cyclohexylamine groups assume an anti conformation. The Pt_2I_2 rhomb is subtly distorted by the relative trans influence of the ligands comprising the coordination sphere of each metal center. The bridging Pt–I bond that is trans to a terminal iodide is 2.5947(2) Å, compared to the 2.5939(3) Å bond that is trans to the cyclohexylamine ligand. Only two other such iodo-bridged dimers, one with *n*-butylamine ligands and the other with diethylamine ligands, have been structurally characterized [16,18,47]. The primary coordination spheres of these three structures are remarkably similar and overlay almost exactly, as illustrated in Fig. 6.

3.4. Comments on the isomerism and reactivity of $[Pt(NH_2C_6H_{11})I(\mu\text{-}I)]_2$

Under microscopic investigation, all the crystals of $[Pt(NH_2C_6H_{11})I(\mu\text{-}I)]_2\cdot 2(CH_3)_2CO$ that formed were of similar habit and over a dozen crystals mounted and examined had the same unit cell. The crystallization vial did not contain any significant amount of dissolved compound or amorphous material. This result suggests that, if two dimeric species are

present, such as cis and trans isomers, they interconvert, with the crystalline form of the trans isomer acting as a thermodynamic sink.

The ability of the two isomers of the dimer to interconvert was probed by variable temperature (VT) NMR spectroscopy. The two peaks in the ^{195}Pt NMR spectrum of the dimer do not appear to arise from species that interconvert rapidly on the NMR time scale. At elevated temperatures, there was no appreciable line broadening, let alone coalescence, of the two signals (Fig. S3a). When compared to room temperature spectra, those acquired at low temperature did not reveal any change in the relative intensities of the signals (Fig. S1). This result indicates that, if the signals arise from two species in dynamic, albeit slow, equilibrium, then they must have identical or very similar energies. Although the crystallographic result described above suggests that the solid state structure of the acetone solvate of the trans isomer is more thermodynamically stable than the solid state structure of the cis dimer, it has no direct bearing on the relative energies of the cis and trans isomers in solution.

Strong support for the interconversion of the two species in solution comes from chromatographic experiments. Analytical thin layer chromatography (TLC) using silica gel resolved a spot corresponding to the dimer into two bands of equal intensity; no development was needed because of the intense red-brown color of the compound. A mobile phase of 1:5 ethylacetate/hexanes produced bands with R_f values of 0.33 and 0.63. Preparative TLC of the material allowed for isolation of these bands. Reanalysis of each of the isolated fractions by analytical TLC again produced two spots of equal intensity with R_f values of 0.33 and 0.63. ^{195}Pt NMR spectra of both isolated fractions show the same two signals that were present before separation (data not shown).

As described in Section 3.2, prior analyses of the reaction of the dimer with NH_3 suggested that the compound existed solely as the trans isomer because *cis*-$[Pt(NH_3)(NH_2C_6H_{11})I_2]$ was exclusively obtained upon reaction with NH_3 [14,21]. It is possible that the two forms of the dimer interconvert and that the trans dimer reacts to afford the cis mononuclear compound. In this scenario, the reaction would proceed to completion owing to continual conversion of cis dimer to the trans dimer in order to maintain equilibrium concentrations of the two. A simpler explanation is available, however. The earlier reports implied that reaction of the dimer with an amine resulted in simultaneous cleavage of both iodide bridges as depicted in Fig. 2 [14,15]. A reanalysis of the reaction mechanism involving a step-wise mechanism (Fig. 7) clearly shows that either of the two dimer isomers can exclusively produce *cis*-$[Pt(NH_3)(NH_2C_6H_{11})I_2]$. As described in Section 3.2, the variable amounts of *trans*-$[Pt(NH_3)(NH_2C_6H_{11})I_2]$ that have been previously reported [35] to form during this reaction are believed to arise from isomerization of the *cis*-$[Pt(NH_3)(NH_2C_6H_{11})I_2]$ over the course of the extended reaction times used.

4. Conclusions

Taken together, these data provide a clearer picture of the nature of the iodo-bridged dimers that are key intermediates in the preparation of mixed ammine/amine platinum(II) complexes. The iodo-bridged dimer studied here is an intermediate en route to the Pt(IV)

prodrug satraplatin, which has been investigated extensively in clinical settings. Reaction of *cis*-[Pt($NH_2C_6H_{11}$)$_2$I$_2$] with acid protonates one of the cyclohexylamine ligands, inducing ligand dissociation and subsequent dimerization via bridging iodide ligands. The dimerization could occur such that the remaining cyclohexylamine ligands are disposed cis or trans to one another across the dimer interface. Both isomers form, which explains the two ^{195}Pt NMR signals, but spectroscopic and chromatographic experiments reveal that the two interconvert. This interconversion has thus far hampered the ability to characterize the isomers in isolation but the apparent thermodynamic preference for crystallization of the acetone solvate of the trans dimer has permitted analysis of its crystal and molecular structure. New mechanistic reasoning provided here establishes a rationale for the formation of *cis*-[Pt($NH_2C_6H_{11}$)$_2$I$_2$] from either of the two dimer isomers, contrary to previous analyses. Moreover, the reported synthetic strategies to access and subsequently use [Pt(Am)I(μ-I)]$_2$ occur orders of magnitude more rapidly than the analogous reactions in aqueous suspension without the formation of side products. It is anticipated that this synthetic approach will facilitate further exploration of compounds bearing a *cis*-amineammineplatinum fragment.

Supplementary Material

Refer to Web version on PubMed Central for supplementary material.

Acknowledgments

This work is supported by the NCI under grant CA034992.

References

[1]. Rosenberg B, VanCamp L, Trosko JE, Mansour VH. Nature. 1969; 222:385. [PubMed: 5782119]

[2]. Hall, MD.; Dolman, RC.; Hambley, TW. Metal Ions in Biolgical Systems. Marcel Dekker; New York: 2004. Platinum(IV) Anticancer Complexes. Vol 42: Metal Complexes in Tumor Diagnosis and as Anticancer Agents

[3]. Johnstone TC, Wilson JJ, Lippard SJ. Inorg. Chem. 2013; 52:12234. [PubMed: 23738524]

[4]. Wheate NJ, Walker S, Craig GE, Oun R. Dalton Trans. 2010; 39:8113. [PubMed: 20593091]

[5]. Sternberg CN, Petrylak DP, Sartor O, Witjes JA, Demkow T, Ferrero J-M, Eymard J-C, Falcon S, Calabrò F, James N, Bodrogi I, Harper P, Wirth M, Berry W, Petrone ME, McKearn TJ, Noursalehi M, George M, Rozencweig M. J. Clin. Oncol. 2009; 27:5431. [PubMed: 19805692]

[6]. Anderson WK, Quagliato DA, Haugwitz RD, Narayanan VL, Wolpert-DeFilippes MK. Cancer Treat. Rep. 1986; 70:997. [PubMed: 3731155]

[7]. Kelland LR, Murrer BA, Abel G, Giandomenico CM, Mistry P, Harrap KR. Cancer Res. 1992; 52:822. [PubMed: 1737343]

[8]. Kelland LR, Abel G, McKeage MJ, Jones M, Goddard PM, Valenti M, Murrer BA, Harrap KR. Cancer Res. 1993; 53:2581. [PubMed: 8388318]

[9]. Žák F, Turánek J, Kroutil A, Sova P, Mistr A, Poulová A, Mikolin P, Žák Z, Kašná A, Záluská D, Neča J, Šindlerová L, Kozubík A. J. Med. Chem. 2004; 47:761. [PubMed: 14736257]

[10]. Holford J, Sharp SY, Murrer BA, Abrams M, Kelland LR. Br. J. Cancer. 1998; 77:366. [PubMed: 9472630]

[11]. Ciuleanu T, Samarzjia M, Demidchik Y, Beliakouski V, Rancic M, Bentsion DL, Orlov SV, Schaeffler BA, De Jager RL, Breitz HB. J. Clin. Oncol. 2010; 28:7002.

[12]. Bagrova SG. Vopr. Onkol. 2001; 47:752. [PubMed: 11826504]

[13]. Giandomenico CM, Abrams MJ, Murrer BA, Vollano JF, Rheinheimer MI, Wyer SB, Bossard GE, Higgins JD III. Inorg. Chem. 1995; 34:1015. [PubMed: 20000850]

[14]. Rochon FD, Kong PC. Can. J. Chem. 1986; 64:1894.

[15]. Khokhar AR, Deng Y, Al-Baker S, Yoshida M, Siddik ZH. J. Inorg. Biochem. 1993; 51:677. [PubMed: 8409984]

[16]. Danzeisen O, Rotter HW, Thiele G. Z. Anorg. Allg. Chem. 1998; 624:763.

[17]. Rochon FD, Masserweh G, Nédélec N. Inorg. Chim. Acta. 2003; 346:197.

[18]. Rochon FD, Buculei V. Inorg. Chim. Acta. 2005; 358:3919.

[19]. van Rijt S, van Zutphen S, den Dulk H, Brouwer J, Reedijk J. Inorg. Chim. Acta. 2006; 359:4125.

[20]. Rochon FD, Bonnier C. Inorg. Chim. Acta. 2007; 360:461.

[21]. Khokhar AR, Deng YJ, Albaker S, Yoshida M, Siddik ZH. J. Inorg. Biochem. 1993; 51:677. [PubMed: 8409984]

[22]. Talman EG, Brüning W, Reedijk J, Spek AL, Veldman N. Inorg. Chem. 1997; 36:854.

[23]. Bruker. APEX2. Bruker AXS Inc.; Madison, Wisconsin: 2008.

[24]. Bruker. SAINT: SAX Area-Detector Integration Program. Bruker AXS Inc.; Madison, Wisconsin: 2008.

[25]. Bruker. SADABS: Area-Detector Absorption Correction. Bruker AXS Inc.; Madison, Wisconsin: 2001.

[26]. Bruker. XPREP. Bruker AXS Inc.; Madison, Wisconsin: 2008.

[27]. Sheldrick, GM. SHELXTL-97. University of Göttingen; Göttingen, Germany: 2000.

[28]. Sheldrick GM. Acta Crystallogr. Sect. A. 2008; 64:112. [PubMed: 18156677]

[29]. Müller P. Crystallogr. Rev. 2009; 15:57.

[30]. Spek AL. J. Appl. Crystallogr. 2003; 36:7.

[31]. Spek, AL. PLATON, A Multipurpose Crystallographic Tool. Utrecht University; Utrecht, The Netherlands: 2008.

[32]. Connelly, NG.; Damhus, T.; Hartshorn, RM.; Hutton, AT. Nomenclature of inorganic chemistry. Royal Society of Chemistry Publishing/IUPAC; Cambridge, UK: 2005. IUPAC recommendations 2005

[33]. Moss GP. Pure Appl. Chem. 1996; 68:2193.

[34]. Johnstone TC, Lippard SJ. Polyhedron. 2013; 52:565. [PubMed: 23554544]

[35]. Rochon FD, Titouna H. Inorg. Chim. Acta. 2010; 363:1679.

[36]. Rochon FD, Buculei V. Inorg. Chim. Acta. 2005; 358:2040.

[37]. Danzeisen OF, Goanta M, Rotter HW, Thiele G. Inorg. Chim. Acta. 1999; 287:218.

[38]. Rochon FD, Buculei V. Inorg. Chim. Acta. 2004; 357:2218.

[39]. Oksanen A, Kivekäs R, Lumme P, Valkonen J, Laitalainen T. Acta Crystallogr. Sect. C. 1989; 45:1493.

[40]. Zimmermann W, Galanski M, Keppler BK, Giester G. Inorg. Chim. Acta. 1999; 292:127.

[41]. Rochon FD, Beauchamp AL, Dion C. Inorg. Chim. Acta. 2009; 362:3885.

[42]. Pažout R, Housková J, Dušek M, Maixner J, Kačer P. Struct. Chem. 2011; 22:1325.

[43]. Sachinvala ND, Chen H, Niemczura WP, Furusawa E, Cramer RE, Rupp JJ, Ganjian I. J. Med. Chem. 1993; 36:1791. [PubMed: 8510107]

[44]. Klement U, Range KJ, Gust R. Z. Kristallogr. 1996; 211:970.

[45]. Oksanen A, Kivekäs R, Lumme P, Laitalainen T. Acta Crystallogr. Sect. C. 1991; 47:719.

[46]. Johnstone TC. Polyhedron. 2014; 67:429.

[47]. Marsh RE. Acta Crystallogr. Sect. B. 2004; 60:252. [PubMed: 15017100]

Highlights

- A new synthetic approach to preparing and using iodo-bridged platinum(II) dimers
- New method is orders of magnitude faster and avoids common side products
- Interpretation of the dimer cleavage mechanism that reconciles previous debate
- Spectroscopic and crystallographic characterization of $[Pt(NH_2C_6H_{11})I(\mu\text{-}I)]_2$

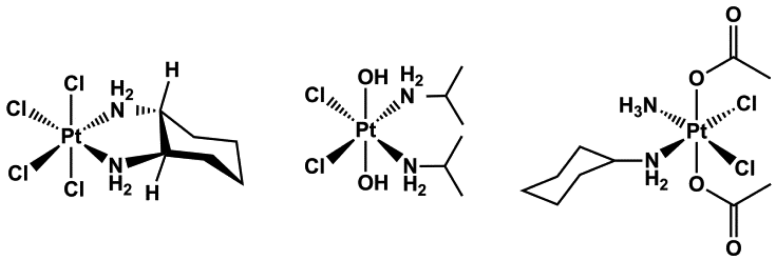

Chart 1.

Platinum(IV) compounds entered into clinical trials.[a]

[a] From left to right: ormaplatin, iproplatin, and satraplatin. Note that ormaplatin was formulated as a racemic mixture of the two possible enantiomers of the compound bearing the *trans*-1,2-diaminocyclohexane ligand [6].

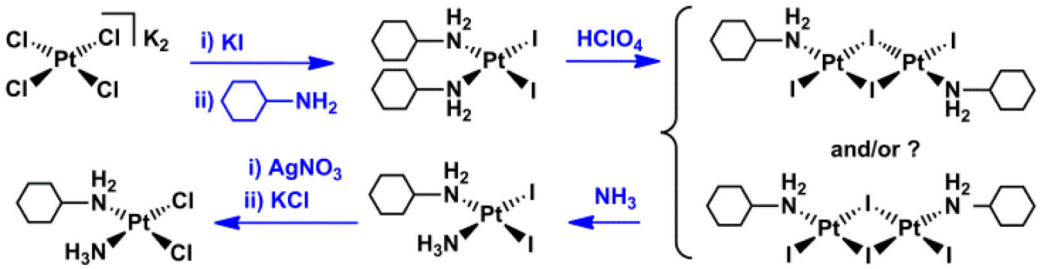

Scheme 1.

The previously reported [14] strategy to synthesize mixed amine/ammine complexes via iodo-bridged dimers.

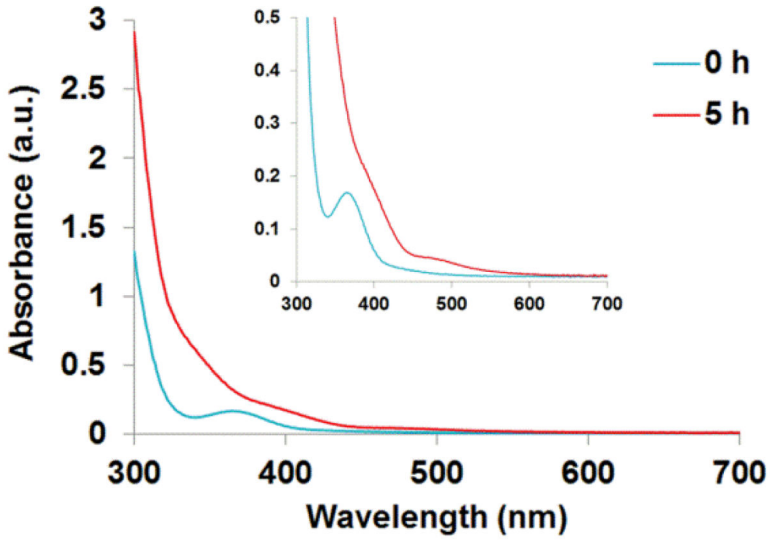

Fig. 1.

UV-vis spectrum of the reaction of *cis*-[Pt($NH_2C_6H_{11}$)$_2$$I_2$] with HBF_4 in acetone showing the growth of bands at approximately 345, 410, and 490 nm. The inset highlights the growth of the low energy features (color available online).

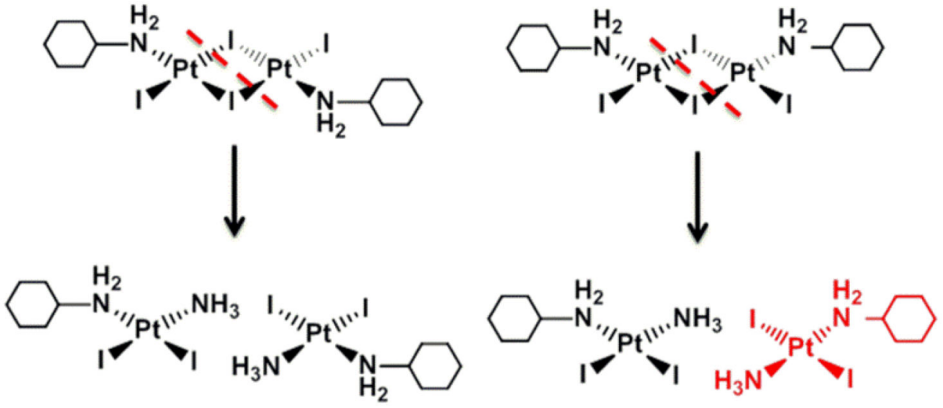

Fig. 2.

Previously proposed cleavage routes of the iodo-bridged dimer. The desired and observed cis product is shown in black and the undesired trans product is shown in red. The red dashed line indicates the proposed cleavage of the dimer effected by NH_3 (color available online).

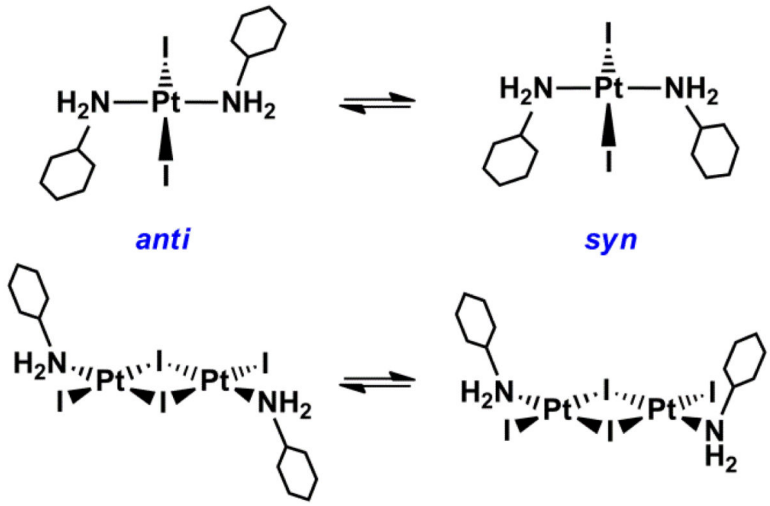

Fig. 3.

Schematic depiction of the conformational isomerism that could be present in $[Pt(NH_2C_6H_{11})I(\mu\text{-}I)]_2$ analogous to that present in *trans*-$[Pt(NH_2C_6H_{11})_2I_2]$.

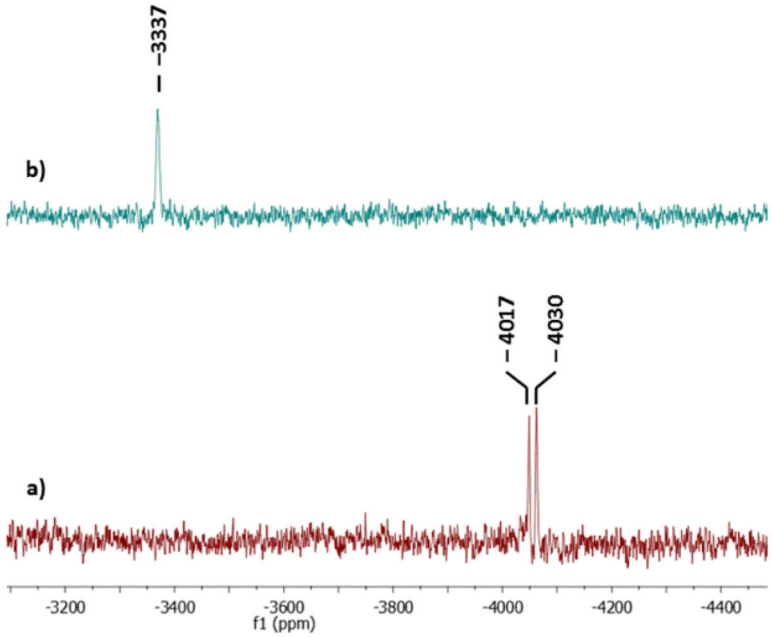

Fig. 4.

^{195}Pt NMR (108 MHz, acetone-d_6) spectra of $[Pt(NH_2C_6H_{11})I(\mu\text{-}I)]_2$ before (a) and after (b) addition of 1 drop of concentrated aqueous ammonia.

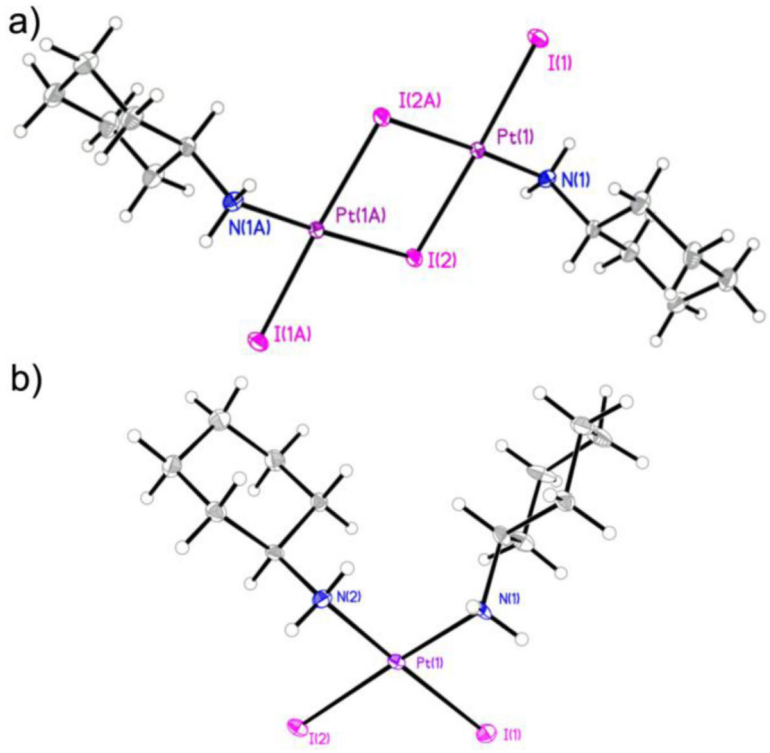

Fig. 5.

Molecular structures of (a) $[Pt(NH_2C_6H_{11})I(\mu\text{-}I)]_2$ and (b) *cis*-$[Pt(NH_2C_6H_{11})_2I_2]$ as determined by X-ray diffraction methods with thermal ellipsoids shown at the 50% probability level. Color code: Pt purple, I magenta, N blue, C grey, H open spheres of arbitrary radius (color available online).

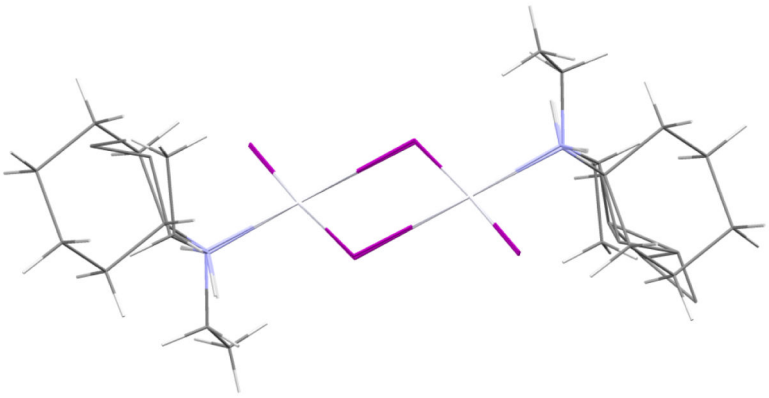

Fig. 6.

Overlay of dimers from the crystal structures of $[Pt(NH_2C_6H_{11})I(\mu\text{-}I)]_2$ (this work), $[Pt(NH_2C_4H_9)I(\mu\text{-}I)]_2$ [18], and $[Pt(NH(C_2H_6)_2)I(\mu\text{-}I)]_2$ [16]. Color code: Pt silver, I purple, N blue, C grey, H white (color available online).

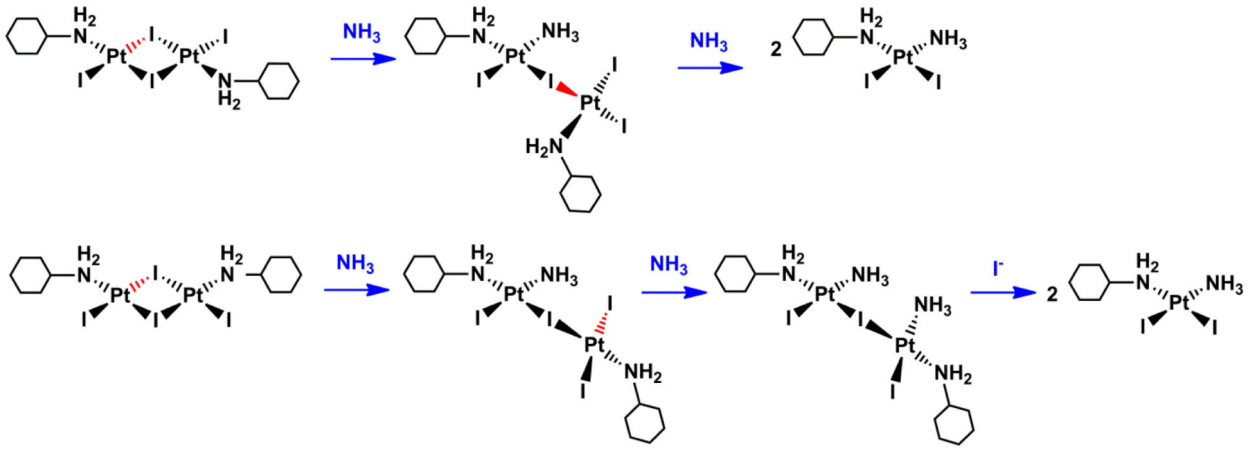

Fig. 7.

Step-wise mechanism for the cleavage of *trans*- (top) or *cis*- (bottom) $[Pt(NH_2C_6H_{11})I(\mu\text{-}I)]_2$ with NH_3. The scissile bond at each NH_3 substitution step, dictated by the trans effect, is colored red (color available online).

Table 1

Crystallographic parameters and refinement details.

	***cis*-[Pt($NH_2C_6H_{11}$)$_2$$I_2$]·$(CH_3)_2CO$**	**[Pt($NH_2C_6H_{11}$)I(μ-I)]$_2$·2$(CH_3)_2CO$**
Formula	$C_{15}H_{32}I_2N_2OPt$	$C_{18}H_{38}I_4N_2O_2Pt$
Formula weight	705.32	1212.28
Space group	*P*1	*P*1
a, Å	9.9819(9)	8.0912(4)
b, Å	10.8095(10)	9.1934(5)
c, Å	11.5144(10)	10.6946(6)
α, °	87.1466(12)	76.054(1)
β, °	66.6155(11)	85.749(1)
γ, °	64.9903(11)	68.769(1)
V, Å^3	1022.96(16)	719.60(7)
Z	2	1
T, K	100(2)	100(2)
μ(Mo Kα), mm^{-1}	9.878	14.015
θ range, °	1.95 to 28.34	1.96 to 29.61
total no. of data	20172	15492
no. of unique data	5067	3988
no. of parameters	192	129
completeness (%)	99.1	98.5
R_1[a] (%)	2.59	1.59
wR_2[b] (%)	6.87	3.51
GOF[c]	1.342	1.058

[a] $R1=\Sigma||F_O| - |F_C||/\Sigma|F_O|$.

[b] $wR2= \{\Sigma[w(F_O^2-F_C^2)^2]/\Sigma[w(F_O^2)^2]\}^{1/2}$.

[c] $GOF= \{\Sigma[w(F_O^2-F_C^2)^2]/(n-p)\}^{1/2}$